PHILOSOPHICAL TRANSACTIONS OF THE ROYAL SOCIETY A MATHEMATICAL, PHYSICAL & ENGINEERING SCIENCES

Comparison between Experiment and Theory [and Discussion]

R. J. Bickerton, A. Taroni, M. L. Watkins, J. Wesson and D. C. Robinson

Phil. Trans. R. Soc. Lond. A 1987 **322**, 173-188
doi: 10.1098/rsta.1987.0046

Phil. Trans. R. Soc. Lond. A **322**, 173–188 (1987)
Printed in Great Britain

Comparison between experiment and theory

By R. J. Bickerton, A. Taroni, M. L. Watkins and J. Wesson
JET Joint Undertaking, Abingdon, Oxfordshire OX14 3AE, U.K.

In the idealized theory of toroidal magnetic confinement, the plasma is supposed to be embedded in a nested set of topologically toroidal magnetic surfaces. The plasma is assumed to be stable so that all transport processes, such as thermal conduction, are determined only by Coulomb collisions between the particles. In this paper, we first compare the experimental results with the predictions of this theory. The actual energy transport rate is found to be much higher than that predicted. This is believed to be due to instability processes in the plasma although there remains the possibility that the idealized or classical theory is not complete. The role of electrostatic and of magnetic instabilities is discussed. Finally, the consequences of a simple model, in which the form of the temperature profile is fixed, are discussed.

Introduction

Comparison between theory and experiment in the field of tokamak physics is a very complex topic. At present, theory is unable to predict the observed performance of tokamak systems in basic respects. An observed example is the lack of understanding of the thermal insulation of the plasma and the resulting energy confinement. There is a rigorous and sophisticated theory of the performance expected from tokamaks in the absence of plasma instabilities. We outline this theory and calculate its implications for a particular set of JET parameters. These results are in strong disagreement with those found experimentally. We then discuss briefly the types of plasma instabilities to be expected and their possible influence on the performance of the device. Finally, we discuss the consequences of one particular simplifying assumption, namely that the current profile is controlled by instabilities and limited to functional forms depending only on global discharge characteristics, such as the ratio of the magnetic field due to the plasma current to the externally applied toroidal magnetic field.

Classical tokamak model

In the classical model a set of nested toroidal magnetic surfaces is produced by the combination of three field contributions: the field due to the plasma current; a field predominantly parallel to the major axis of the toroid produced by external coils; and the toroidal field also produced by external coils. In a tokamak, the toroidal component is the largest one. As each magnetic field line winds around the torus it follows a helical path and traces out a toroidal magnetic surface. Both the magnetic field $\boldsymbol{B}$ and the current density $\boldsymbol{j}$ lie in this surface. For a tokamak, small departures from axisymmetry may cause the break up of the surfaces and the formation of separate nested structures called magnetic islands. Large departures may lead to a complete loss of surfaces leaving a volume filled by ergodic field lines (Morozov & Solov'ev 1966). Figure 1 shows the cross section in a meridional plane of a nested

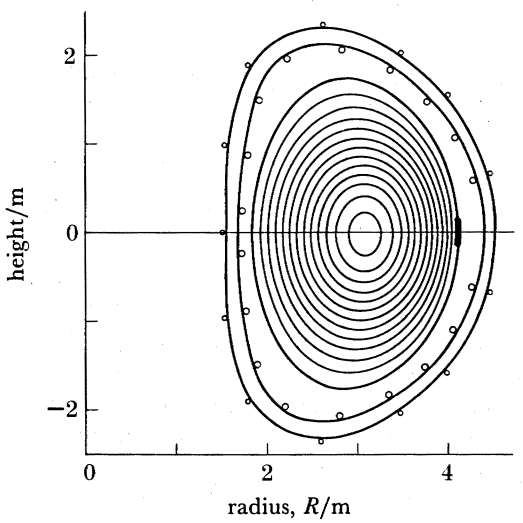

FIGURE 1. Magnetic flux surfaces calculated from magnetic measurements outside the plasma.

set of surfaces deduced from external magnetic field measurements for a particular plasma discharge in JET. The derivation from the measurements *assumes* that such surfaces exist and the figure is shown for illustration, it does not prove their existence.

An isotropic plasma pressure p in such a system is held in equilibrium by the magnetic forces (Spitzer 1956), that is

$$\nabla p = \boldsymbol{j} \times \boldsymbol{B}. \tag{1}$$

Applying this equation to the toroidal set of surfaces described earlier leads to the equation (Shafranov 1957; Laing *et al.* 1959; Grad & Rubin 1958) for toroidal equilibrium, namely

$$\nabla \cdot R^{-2} \nabla \psi = -\mu_0 p'(\psi) - F(\psi) F'(\psi)/R^2, \tag{2}$$

where R is the major radius coordinate, ψ the poloidal flux labelling a magnetic surface, $F = RB_\phi$, B_ϕ being the toroidal component of the magnetic field and the prime denotes differentiation with respect to ψ. Both p and F are surface functions, that is they are constant on a magnetic surface.

In the absence of dissipation, an equilibrium described by (2) would be maintained indefinitely. The existence of dissipative processes, such as energy and particle losses driven by temperature and density gradients, causes the plasma pressure to decay away on the diffusive time scale. However, with suitable sources for energy and particles the plasma can be maintained in steady state.

In the classical theory, plasma convection and heat conduction across magnetic field lines are due entirely to collisions between particles. The simplest example is that of a plasma in plane slab geometry with a density gradient across the magnetic field. The electrons then undergo a random walk in which the characteristic length is the electron gyro-radius, ρ, and the time is the electron–ion collision time τ_e, so the cross-field diffusion coefficient D has the form

$$D \sim \rho^2/\tau_e. \tag{3}$$

Similar expressions can be derived for the thermal diffusivity, χ, and for the electrical resistivity η (Braginskii 1965). In toroidal geometry, the trajectories of the particles are more complex. Because of the variation of field strength on a surface, some particles are 'trapped' in the weaker field on the outer side of the torus. The particles then move in banana-shaped orbits between their reflections at turning points on the surface. These orbits depart from the magnetic surfaces by substantially more than a gyro-radius and the result is to increase significantly the transport coefficients.

An elaborate theory of 'neoclassical' transport has been constructed based on these ideas (Galeev & Sagdeev 1968; Rosenbluth *et al.* 1972; Hazeltine *et al.* 1973; Hazeltine & Hinton 1973). With this as the basis, it is possible to predict the tokamak performance by using the conservation equations, the equilibrium equation and the neoclassical set of transport coefficients. One problem remains, namely the boundary conditions. At the boundary the plasma interacts with the limiters and the wall so that a model is required covering the atomic processes and the resulting energy flow and radiation losses in this outer region. Self-consistent models (Watkins *et al.* 1984) have been developed for this boundary taking into account the flow of plasma along field lines to the limiters in the 'scrape-off' layer and the sputtering of impurities. Combining a model of this type with the neo-classical transport and radiation models for the interior can be said to be the classical model, that is the performance prediction based on a rigorous theory ignoring the effect of any plasma instabilities. The time-dependent behaviour of the plasma can now be calculated by using a computer code to solve the equations as outlined above. The two-dimensional toroidal problem is effectively converted to one dimension through the assumption that parameters such as temperature and density are constant on a magnetic surface. In our calculations, only the principal terms in the neo-classical theory are retained, these include the inward (Ware 1970) particle and thermal fluxes (Hirshman & Sigmar 1981), the neoclassical corrections to resistivity (Hirshman *et al.* 1977), the principal effects of impurities and the ion thermal diffusivity (Chang & Hinton 1985). The bootstrap current (Bickerton *et al.* 1971) is not included.

Model predictions

Before describing the results of the full calculations it is instructive to look at the basic physics described by the neoclassical equations. In this model, the electron-energy transport is negligible and the two principal channels for energy loss are ion thermal conduction and bremsstrahlung radiation. In the steady state, these losses balance the power input.

The ion heat flux is a random walk process in which the step length is the width, w, of the ion orbit in the field and the time step is the ion–ion collision time, τ_{ii}. Thus the corresponding energy confinement time τ_{Ei} takes the form

$$\tau_{Ei} \sim (a/w)^2 \tau_{ii} \propto a^2 T^{\frac{1}{2}} n^{-1} B_\theta^2 \epsilon^{-\frac{1}{2}},$$

where a is the effective minor radius of the plasma, $\epsilon = a/R$, and T is the temperature. The associated power loss per unit volume takes the form for fixed ϵ and safety factor q,

$$P_i \sim n^2 T^{\frac{1}{2}} / (a^2 B_\phi^2).$$

The loss by bremsstrahlung, P_b, has a similar form, $P_b \sim n^2 T^{\frac{1}{2}}$. Combining these losses gives $\tau_\epsilon = 3nT/(P_b + P_i)$, which for the JET parameters considered here of $\bar{n}_e \sim 2 \times 10^{19}$ m^{-3},

$B_\phi = 3.4$ T, $I_p = 3$ MA gives $\tau_\epsilon = 25 T^{\frac{1}{2}} s$, where T is in kiloelectronvolts. In this case the ion thermal conduction and bremsstrahlung losses are comparable. Note that for $T = 1$ keV, $\tau_\epsilon = 25$ s, whereas for 10 keV, $\tau_\epsilon = 80$ s.

For ohmically heated plasmas, the steady-state temperature is determined by the balance between energy loss and ohmic heating, $(= \eta j^2)$. Allowing for neoclassical corrections to the resistivity, the average power density in JET for $Z_{\text{eff}} = 1$ and a current of 3 MA is approximately

$$P_\Omega = 2 \times 10^4 / T^{\frac{3}{2}} \text{ W m}^{-3}.$$

For the conditions given above, this gives $T \sim 7$ keV and $\tau_\epsilon \sim 60$ s. These values are of course much higher than the experimental values of $\bar{T}_e \sim 2$ keV and $\tau_\epsilon \sim 0.6$ s.

Turning now to the more complete computer calculations, we concentrate on a particular JET pulse (as discussed above) with the following parameters: plasma current $I_p = 3$ MA; toroidal field $B_\phi = 3.4$ T; minor plasma radius $a_p = 1.1$ m; elongation ratio of the non-circular cross section $b/a = 1.5$ and $\bar{n}_e = 2.1 \times 10^{19}$ m^{-3}. The measured electron-temperature profile and density profile are shown in figure 2. Other measured parameters, such as effective ion charge, Z_{eff}, central electron and ion temperatures, ohmic input power and global energy confinement time τ_ϵ, are listed in table 1. The profiles and parameters are for 11 s into the pulse, by which time steady-state conditions have been established in the experiment.

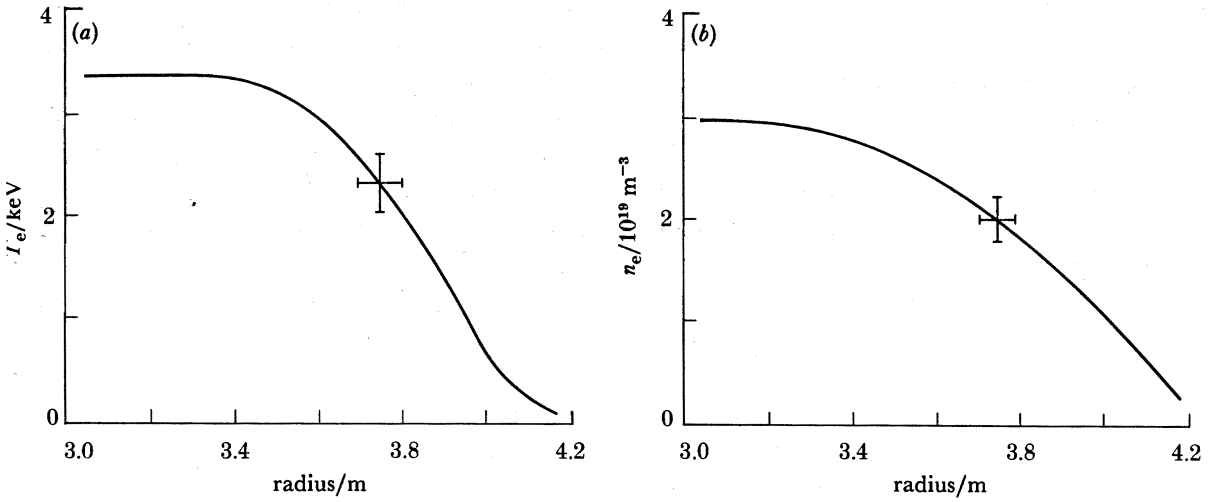

FIGURE 2. Electron-temperature and electron-density measurements along the major radius. Pulse no. 3844, $t = 11$ s.

TABLE 1. MODEL

χ_e	χ_i	Z_{eff}	sawteeth	time/s	T_e/keV	T_i/keV	τ_ϵ/s	P_Ω/MW
experiment		3	yes	11	3.4	2.4	0.5	2.1
0	$1 \times$ NC	1	no	98	14.6	14.1	71	0.12
0	$1 \times$ NC	1	yes	4	6.5	5.9	53	0.3
0	$1 \times$ NC	1	yes	138	15.9	15.4	80	0.1
0	$1 \times$ NC	3	yes	4	6.2	5.5	5.6	0.8
0	$1 \times$ NC	3	yes	16	7.3	6.8	6.4	0.65
CMG	$5 \times$ NC	3.3	yes	4	3.3	2.5	0.66	2.2

The neoclassical electron thermal diffusivity is negligible compared with the ion value. In the computations it is put equal to zero.

PHILOSOPHICAL TRANSACTIONS OF THE ROYAL SOCIETY A MATHEMATICAL, PHYSICAL & ENGINEERING SCIENCES

The predictions of detailed calculations with the neoclassical model described above are shown in figure 3 and the corresponding parameters are listed in table 1. A steady state is reached only after a time of more than 100 s. Consequently, in short duration of the experiment, the temperatures reached in the calculations are determined simply by the thermal capacity of the plasma.

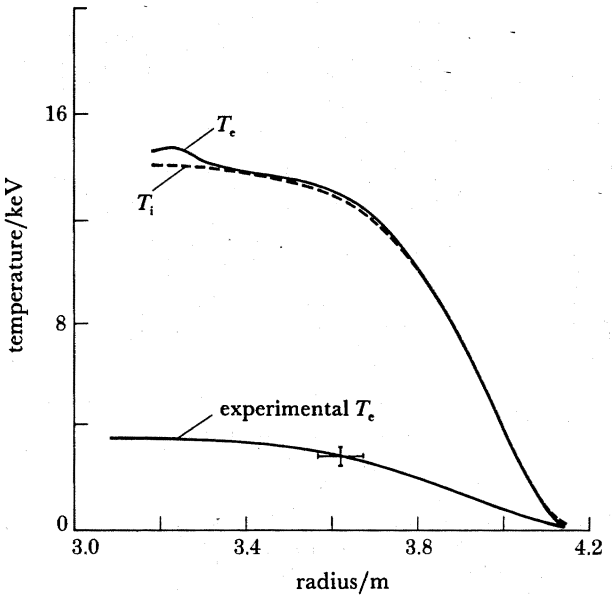

FIGURE 3. Neoclassical computations of the electron and ion temperatures compared with the measured electron temperature along the major radius. Pulse time for experiment is 11 s, pulse time for computations is 98 s (see table 1).

A key feature of the experimental results is the evidence for so-called sawtooth oscillations in the electron temperature in the central region of the discharge. Figure 4 shows typical sawtooth behaviour for such a discharge. There is abundant evidence from JET and other tokamaks that this is due to a gross instability localized around the plasma centre. In studying stability, linear displacements are assumed to take the form,

$$\zeta = \zeta(r)\ \exp \mathrm{i}(m\theta - n\phi), \tag{4}$$

where θ and ϕ are the poloidal and toroidal angles. An instability is resonant with the local field lines when

$$m/n = q(r), \tag{5}$$

where q is the so-called safety factor ($= B_\phi r/B_\theta R$). At such a resonance, the perturbations and the local field lines have the same spiral pitch in passing round the machine. This minimizes the field perturbation caused by the displacement, so making instability energetically more likely. The parameter q normally decreases toward the centre of the plasma. When the central value falls below unity, a $q = 1$ resonance appears leading to the possibility of an $m = 1, n = 1$ instability. The sawtooth oscillations are widely assumed to be the nonlinear consequence of this instability. Qualitative nonlinear models have been developed for example by Kadomtsev (1975) and Wesson (1986). Although the models differ in important details, their overall effect

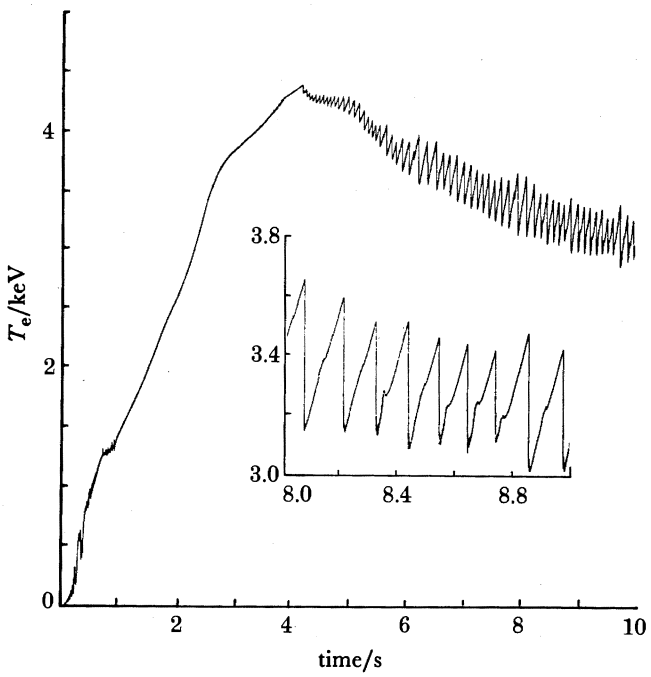

FIGURE 4. Temporal variation of the central measurement of the electron temperature, showing the 'sawtooth' behaviour.

is similar. Essentially the current density on the axis has a tendency to rise due to the proportionality between the electrical conductivity σ and the electron temperature, $\sigma \propto T_e^{\frac{3}{2}}$. The rising current density takes q in the central region to values less than 1. At some critical value, the resulting $m = 1$, $n = 1$ instability exchanges hot plasma and flux close to the axis with colder plasma and the same flux from outside this region. The resultant is a series of relaxation oscillations which flatten the average current density and temperature profiles to maintain $q \sim 1$ in the centre.

Thus, the next step in the prediction work is to add the effects of this gross instability to the classical model. We then have three radial zones: the central one dominated by sawteeth; an intermediate zone, where transport phenomena are dominant; and the outer zone near the wall where atomic processes and plasma surface interactions such as the sputtering of impurities are important. Figure 5 shows this subdivision.

The predictions when the sawtooth behaviour is added are shown in figure 6 and the resulting parameters are included in table 1. The flattening of the temperature profile is evident. However, the predicted energy confinement time still greatly exceeds the experimental value and the ohmic input is only *ca.* 100 kW compared with 2 MW for the experiment. One result of the low power input is that the self-consistent boundary model gives a very low impurity sputtering rate so that the effective ion charge Z_{eff} is *ca.* one rather than three as in the experiment. If Z_{eff} is artificially increased to three in the calculations, then the energy confinement time is reduced from 80 s to 6.4 s. The resulting profiles are shown in figure 7. This change reflects an order of magnitude increase in the dominant energy transport coefficient, namely the ion thermal diffusivity. The increase comes about because of the increased collision rate and the lower ion temperature.

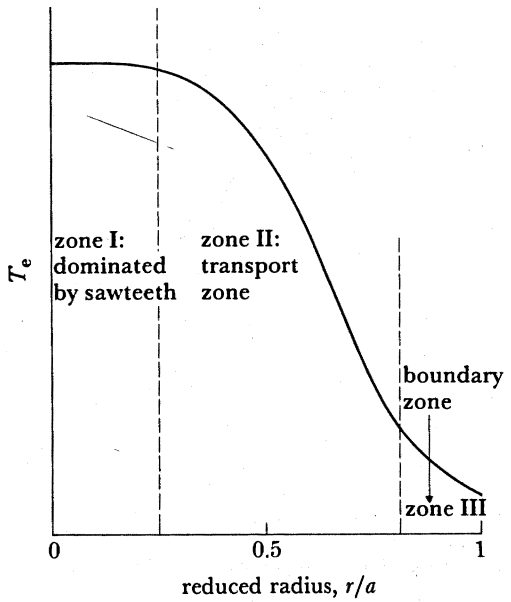

FIGURE 5. Schematic diagram showing the three zones into which the plasma may be divided.

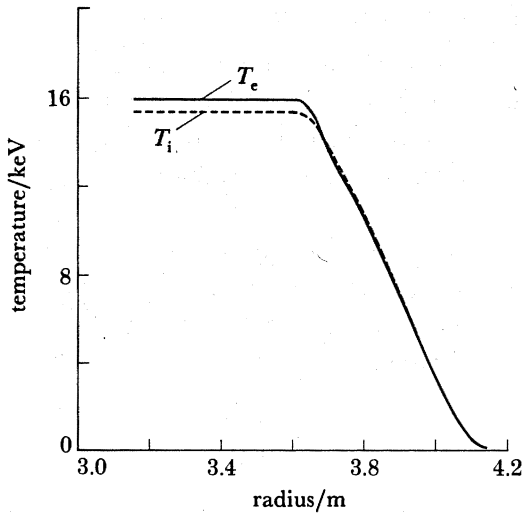

FIGURE 6. Calculated neoclassical electron and ion temperature profiles including a 'sawtooth' model. Pulse time is 138 s.

The experiments in many tokamaks including JET show that the plasma resistivity for toroidal currents is close to the theoretical value, which is either classical or neoclassical according to the degree of electron trapping. In the case of JET with its tight aspect ratio, the proportion of trapped electrons is high. Consequently, the difference between neoclassical and classical resistivity is significant. The best agreement between the Z_{eff} deduced from resistivity and that measured spectroscopically is obtained if the neoclassical value is used (Christiansen *et al.* 1985). This has therefore been used in the modelling calculations described above.

PHILOSOPHICAL TRANSACTIONS OF THE ROYAL SOCIETY A MATHEMATICAL, PHYSICAL & ENGINEERING SCIENCES

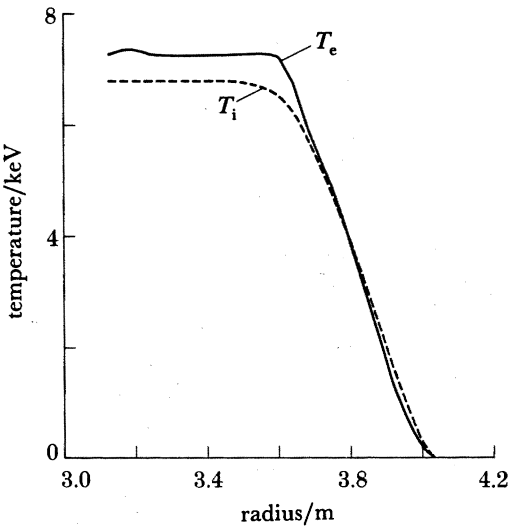

FIGURE 7. Neoclassical electron- and ion-temperature profiles including a 'sawtooth' model and impurity effects. Pulse time is 16 s (see table 1).

INSTABILITIES AND TRANSPORT

We see that, with transport determined only by collisions, provision for impurities and a model for the gross sawtooth instability in the centre, the calculated confinement time is about an order of magnitude larger than in the experiment (6.4 s instead of 0.63 s). The additional transport is probably due to the effect of plasma instabilities. These can be divided into two distinct classes.

In one class, the structure of nested magnetic surfaces is essentially undisturbed, but density fluctuations are destabilized by the gradients in temperature and density to produce 'drift-wave' instabilities (Kadomtsev 1965). The presence of trapped particles further de-stabilizes such waves. The basic drift-wave frequency ω is

$$\omega \approx k_\perp \frac{T_e}{eB} \frac{1}{n} \frac{dn}{dr}, \tag{6}$$

where $k_\perp$ is the wavenumber perpendicular to the magnetic field and it is assumed that the parallel wavenumber $k_\parallel \ll k_\perp$. These waves involve electrostatic potential fluctuations and oscillatory motion of the plasma ions across the magnetic field. Nonlinear considerations lead to transport coefficients of the form,

$$\chi \sim \gamma / k_\perp^2, \tag{7}$$

where γ is the linear growth rate. Calculations of γ and $k_\perp$ for the cases where there is a significant trapped-particle population lead to the result

$$\chi \propto T_e^\alpha,$$

where α ranges from $-\frac{1}{2}$ to $+\frac{5}{2}$, depending on the ratio of collision frequency to the bounce frequency between mirror turning points (Kadomstev & Pogutse 1971). Evidently, drift-wave induced transport generally has a most unfavourable temperature dependence in comparison

with neoclassical transport. The presence of drift-wave type density fluctuations inside tokamak plasmas has been confirmed by experiments in which radiation from an active probing beam is scattered from the perturbations. However, the fluctuating electric fields inside the hot plasma have not been measured and so the resulting transport cannot be unambiguously determined. Liewer (1985) has given a comprehensive review of this subject.

The other basic class of instability receives its energy from the plasma current. These magnetohydrodynamic instabilities break up the magnetic surfaces. In the extreme case, a field line may explore the entire plasma volume, connecting the centre of the plasma to the wall. An example is shown in figure 8. Because the ratio of classical electron thermal diffusivity along and across field lines is typically 10^{12}–10^{14} in JET plasmas, it is clear that only a small random radial component of magnetic field is required to give significant radial transport (Rechester & Stix 1976; Rechester & Rosenbluth 1978). Again, it is not possible to measure the magnetic-field fluctuations inside the plasma with the required precision. Fluctuations in magnetic field outside the plasma are measured and usually they correspond to low m-number modes inside the plasma or to high m-number modes near the surface. This shows that some magnetohydrodynamic activity is taking place but does not allow a quantitative determination of the resulting losses.

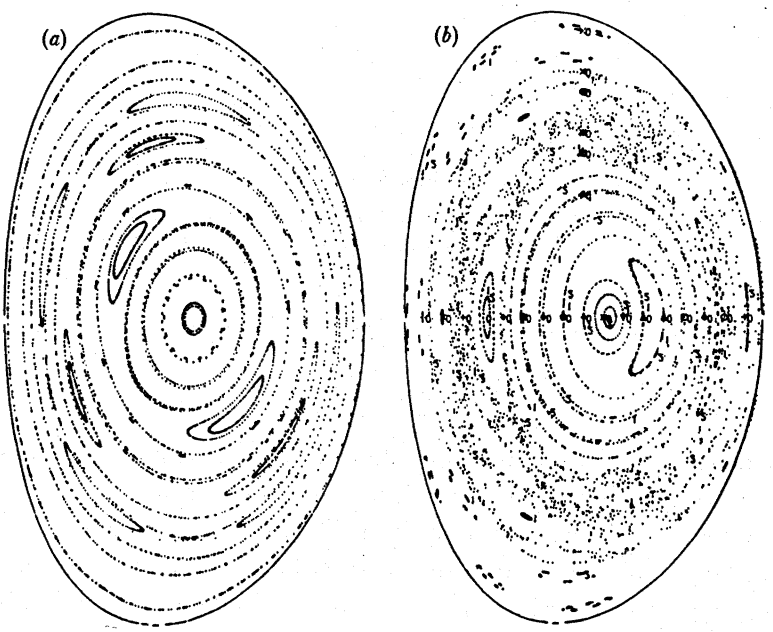

FIGURE 8. Magnetic field lines exhibiting (*a*) closed magnetic surfaces and (*b*) ergodic behaviour.

PROFILE CONSISTENCY AND BOUNDARY CONDITIONS

A definitive theory of the various instabilities and their nonlinear consequences has not yet been developed. A particular problem is the wide variety of experimental results which are difficult to explain on the basis of a single mechanism. Recently, it has become increasingly clear that profiles of temperature and current density tend to evolve towards constant forms (Coppi 1980). That is

$$T_e(r) = T_0 f_1(r, q_a), \tag{8}$$

PHILOSOPHICAL TRANSACTIONS OF THE ROYAL SOCIETY A MATHEMATICAL, PHYSICAL & ENGINEERING SCIENCES

where q_a is the safety factor at the plasma boundary. This is demonstrated in figure 9, where JET electron-temperature profiles for a particular narrow range of q_a show a constant profile of $T_e(r)/T_0$. Similar results are obtained over the whole range of q_a. For classical resistivity, which is only a function of electron temperature and Z_{eff}, the steady-state (constant electric field) current density takes the form

$$j(r) = j_0 f_2(r, q_a, Z_{eff}). \tag{9}$$

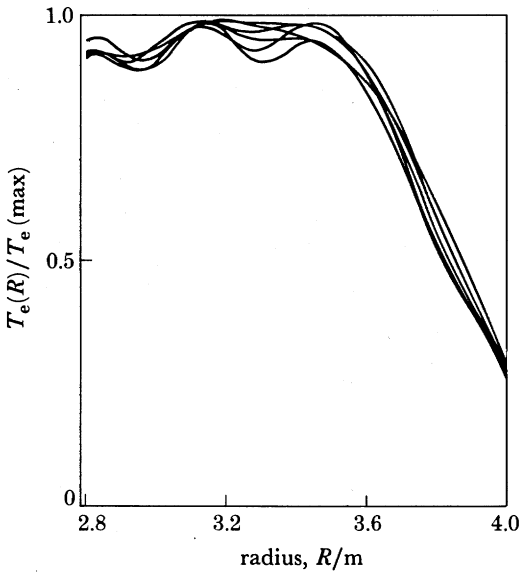

FIGURE 9. Six normalized profiles of electron temperature illustrating the concept of 'profile consistency' (2 keV < T_e(max) < 3.5 keV). $B_T = 3.4$ T, $I_p = 4.0$ MA.

The neoclassical resistivity depends on the density and the local aspect ratio (R/r) so that in this case

$$j(r) = j_0 f_3(r, q_a, Z_{eff}, n). \tag{10}$$

In all tokamaks, the electron temperature profile is measured with greater precision than the current profile, indeed the latter is normally derived from the former using the deduced local electric field and resistivity. However, analysis of the transient behaviour of discharges such as $T-10$ (Kadomtsev 1986) suggest that the current density is the primary parameter which is forced into a fixed profile, the electron temperature profile adjusting to give this current profile. Thus the experiments seem consistent with the concept that for a given aspect ratio and q_a, there is one preferred radial profile of current density. Near the axis, the current density is limited by the sawtooth instability.

The most obvious explanation for such current profile constancy is that it represents a state of marginal stability against magnetohydrodynamic modes. Linear MHD stability analysis for resistive tearing instabilities can be carried out in the cylindrical approximation (Furth *et al.* 1973). Nonlinear analysis of the unstable modes is also possible (Turner & Wesson 1982) and predicts that under normal conditions magnetic islands grow to limited extent and then saturate, flattening both current and temperature gradients near the resonant surfaces.

Application of this analysis to the most relevant 'classical' profile from our simulations,

namely that with $\chi_i = 1 \times$ neoclassical, $Z_{eff} = 3$ and the sawtooth model incorporated shows it to be stable against all modes. The experimental profile analysed in the same way is found to be weakly unstable to the $m = 2$ mode, leading only to a relatively narrow island. Thus it seems that tearing modes of this type affect the transport only marginally.

These results show that we cannot explain the current profile consistency on the basis of simple tearing mode theory. It may be that microtearing modes driven by the combination of current flow and the electron temperature gradient are responsible (see Drake *et al.* 1980; Rebut & Brusati 1986).

We now follow the assumption that the current density profile in a tokamak will be controlled so that it always takes up a particular form. The thermal electron transport is then *determined* by this profile together with the energy sources and not by local conditions. Up to some limit, the profile remains unaffected by changes in the radial distribution of input power such as those due to the application of additional heating.

One example of such an 'anomalous' electron thermal diffusivity is that derived by Coppi & Mazzucato (1979) and modified by Gruber (1982) under the assumption that 'consistent' profiles of current density and temperature develop. For the case $j = j_0 \exp(-\alpha r^2/a^2)$ and ohmic discharges the thermal diffusivity is given by

$$\chi_e = 5 \times 10^{15} \frac{aB_\theta}{A^{\frac{1}{2}} r n_e^{\frac{4}{5}} T_e} \text{ m}^2 \text{ s}^{-1},$$

where a is the minor radius of the plasma, B_θ the poloidal magnetic field and A is the atomic number. The Coppi–Mazzucato–Gruber coefficient has been used for the simulation of ohmic discharges in several tokamaks, including JET, with adjustments (*ca.* $\pm 50\%$ of the numerical coefficient).

For JET, this coefficient, together with neoclassical χ_i enhanced by a factor 3–5, neoclassical

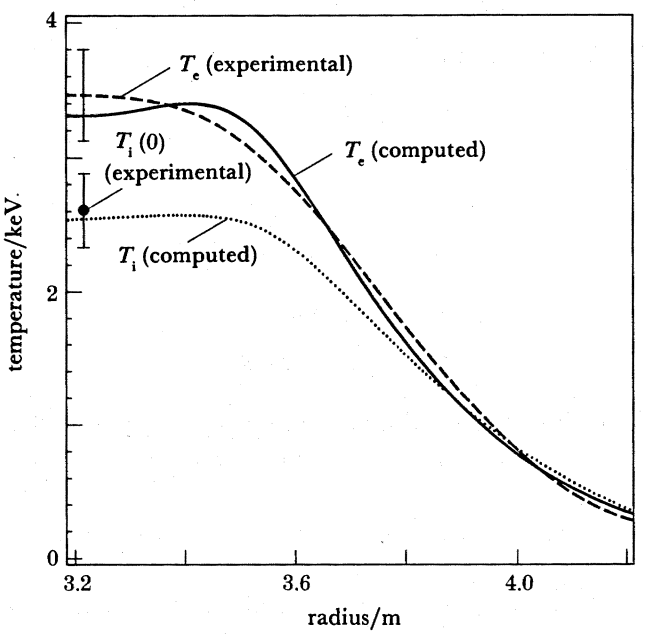

FIGURE 10. Experimental measurements of the electron and ion temperature compared with profiles computed by using anomalous transport together with a 'sawtooth' and impurity model.

resistivity, and the sawtooth and boundary models previously described, does allow a good simulation of ohmic discharges. Simulation results for the shot considered above are given in figure 10 and table 1.

Profile consistency and confinement scaling

In a steady state where the current is inductively driven, there will be a fixed electron-temperature profile corresponding to the current density profile. If we make the simplifying assumption of a fixed electron density profile, we see that with profile consistency the entire electron-energy content in the plasma depends only on the temperature at the boundary T_b. This boundary temperature is determined by the power handling capacity of the mechanisms in the scrape-off layer which convey the power to the limiter or divertor.

We now give a simplified calculation of the consequences of this model. In particular, we shall determine the parametric dependence of the energy confinement time $\tau_E = W/P$, where W is the total energy content of the plasma and P is the total power input. The heat flux ϕ through the boundary is

$$\phi = P/S,$$

where S is the surface area. Because the average temperature is proportional to T_b, the total energy content of the plasma,

$$W \propto VnT_b,$$

where V is the plasma volume. Thus the global confinement time

$$\tau_\epsilon \propto VnT_b/S\phi.$$

If we assume that the heat flux has the dependence $\phi \propto n_b T_b^\alpha$, $n_b \propto n$ then

$$\tau_\epsilon \propto Vn^{(\alpha-1)/\alpha} P^{-(\alpha-1)/\alpha} S^{1/\alpha}.$$

Taking $V \propto Ra^2$ and $S \propto Ra$ we obtain

$$\tau_\epsilon \propto R^{(\alpha-1)/\alpha} a^{(2\alpha-1)/\alpha} n^{(\alpha-1)/\alpha} P^{(1-\alpha)/\alpha} \tag{11}$$

and for various α this gives

$$\alpha = 1 \rightarrow \tau_\epsilon \propto R^0 a n^0 P^0,$$

$$\alpha = \tfrac{3}{2} \rightarrow \tau_\epsilon \propto R^{\frac{1}{3}} a^{\frac{4}{3}} n^{\frac{1}{3}} P^{-\frac{1}{3}},$$

$$\alpha = 2 \rightarrow \tau_\epsilon \propto R^{\frac{1}{2}} a^{\frac{3}{2}} n^{\frac{1}{2}} P^{-\frac{1}{2}},$$

$$\alpha = 3 \rightarrow \tau_\epsilon \propto R^{\frac{2}{3}} a^{\frac{5}{3}} n^{\frac{2}{3}} P^{-\frac{2}{3}}.$$

These scalings show that, if the thermal flux in the scrape-off region depends to any higher power of the boundary temperature than unity, then there will be confinement degradation as the input power is increased.

This is qualitatively in agreement with observations (Goldston 1984; Duesing & Jacquinot 1986).

We shall now consider the case when the boundary behaviour is determined by the conventional scrape-off model. In this model, the plasma flows to the limiter in a scrape-off layer of thickness, Δ, in a time, τ, which is approximately the sound transit time along the length,

L, to the limiters, that is $\tau \approx L/C_s$, where C_s is the ion sound speed. The power loss at the surface is then

$$P = 3n_b\, T_b(\Delta/\tau)\, 4\pi^2 Ra.$$

Taking the scrape-off thickness to be approximated by the penetration length for neutral atoms, and taking both the neutral velocity and sound speed to be characterized by the ion thermal velocity at the edge, then

$$\phi \propto T_b^2/L. \tag{12}$$

We next consider the case where the only power input is ohmic heating arising from the plasma current, I. If q on axis is limited to unity by the sawtooth behaviour the ohmic heating, $P_\Omega \propto B_\phi I/T^{\frac{3}{2}}$. Equating this to the loss implied by (12), gives the temperature and the consequent energy confinement time as

$$\tau_e \propto \bar{n} qRa \left(\frac{R}{B_\phi^2 a}\right)^{\frac{2}{7}}.$$

This is remarkably similar to the experimental scaling at low density (Bickerton 1986; Gibson this symposium). It should be noted that the scaling relation will change as the essential mechanisms in the scrape-off layer vary from one régime to another. A complete treatment would require a more complex model taking into account energy equipartition between electrons and ions.

In the discussion above, we have assumed that the relevant boundary is the last closed magnetic surface grazing the limiter. For JET-like cases in which there is a significant radiating annulus surrounding the hot plasma, the relevant boundary is probably the radius at which the radiated power per unit volume is equal to the local power input, that is the boundary between zone II and III in figure 5. Again, the temperature here will be determined by the power handling capability of zone III.

Discussion

The profile consistency model described above does not attempt to explain the detailed mechanisms maintaining the constant current profile. (See Kadomtsev, this symposium; Furth 1985, for tentative explanations). We have merely explored the consequences of making the assumption that for each value of q at the boundary there is one preferred current density profile and a corresponding temperature profile. However, the resulting consequences are in qualitative agreement with the following experimental observations on tokamaks including JET.

(*a*) The confinement times and temperature profiles are found to be largely independent of the radial deposition profile of additional heating.

(*b*) In the H-mode, the boundary mechanisms are changed, permitting much higher boundary temperatures for a given power flow and correspondingly increased confinement times.

(*c*) In experiments where the current is non-inductively driven, the confinement time is sometimes higher than otherwise. Essentially, the coupling between electron temperature and current density is removed or at least changed.

(*d*) The importance of the boundary region may explain the variability of results from different devices where the limiter geometry and limiter material vary.

(*e*) The widely observed confinement degradation with additional heating is the natural consequence of the power flow through the boundary increasing faster than linearly with temperature (see Duesing *et al.*, this symposium and Jacquinot *et al.*, this symposium).

(*f*) The model suggests a number of steps to improve confinement. The density at the boundary should be reduced as much as possible to increase the boundary temperature. Pump limiters, divertors and pellet refuelling should therefore lead to improvements. Non-inductive current drive and/or the production of superthermal electrons allow the decoupling of the current density and electron temperature and may permit steeper temperature gradients, while maintaining a constant profile of current density

Conclusions

(*a*) There is a well-developed theory of tokamak performance, in which a nested set of toroidal magnetic surfaces are assumed to exist and transport phenomena are entirely due to binary collisions.

(*b*) The predictions of this theory are in serious disagreement with experiment, the one exception being the plasma resistivity for toroidal current flow.

(*c*) Including a localized internal (sawtooth) instability and taking into account the measured impurity content of the plasma reduces the discrepancy in energy confinement time to about one order of magnitude.

(*d*) The remaining difference is probably accounted for by the effects of either drift wave instabilities or break-up of the magnetic surfaces.

(*e*) The essential poloidal component of magnetic field is produced by the current flow in the plasma itself. If it is assumed that there are optimal profiles of current density set for example by marginal stability, then a number of tokamak properties follow naturally. Many of these properties agree qualitatively with the experimental results.

(*f*) The model focuses attention on conditions in the boundary and suggests a number of ways in which the performance of JET can be improved. Some of these will be tested in the future programme of experiments and modifications.

We are pleased to acknowledge the help of Dr D. Bartlett, Dr M. F. F. Nave and Dr F. Tibone in some aspects of this work.

References

Bickerton, R. J., Connor, J. W. & Taylor, J. B. 1971 *Nature, phys. Sci.* **229**, 110–112.

Bickerton, R. J. 1986 In *12th European Conference on Controlled Fusion and Plasma Physics, Budapest, 2–6 September 1985.* (*Plasma Phys. controlled Fusion* **28**, 55.)

Braginskii, S. I. 1965 *Rev. Plasma Phys.* **1**, 205–311.

Chang, C. S. & Hinton, F. L. 1985 AMPC Report 14-011. (Also *Physics Fluids.* (In the press.))

Christiansen, J. P., Campbell, D. J., Cordey, J. G., Ejima, S. & Lazzaro, E. 1985 Controlled fusion and plasma physics. *In Proc. 12th European Conference on Controlled Fusion and Plasma Physics, Budapest, 2–6 September 1985.* (*Europhysics conference abstracts* **9F** (1), 327.)

Coppi, B. 1980 *Comments Plasma Phys. controlled Fusion* **5**, 261.

Coppi, B. & Mazzucato, E. 1979 *Phys. Lett.* A **71**, 337.

Drake, J. F., Gladd, N. T., Liu, C. S. & Chang, C. L. 1980 *Phys. Rev. Lett.* **44**, 994.

Furth, H. P., Rutherford, P. H. & Selberg, H. 1973 *Physics Fluids* **16**, 1054.

Furth, H. P. 1985 In *12th European Conference on Controlled Fusion and Plasma Physics, Budapest, 2–6 September 1985.* (*Europhysics conference abstracts* **9F** (2), 358.)

PHILOSOPHICAL TRANSACTIONS OF THE ROYAL SOCIETY A MATHEMATICAL, PHYSICAL & ENGINEERING SCIENCES

Galeev, A. A. & Sagdeev, R. S. 1968 *Sov. Phys. JETP* **26**, 233.
Goldston, R. J. 1984 *Plasma Phys. controlled Fusion* **26** (1A), 87.
Grad, H. & Rubin, H. 1958 In *Proc. 2nd UN Conference on Peaceful Uses of Atomic Energy*, vol. 31, p. 190. United Nations.
Gruber, O. 1982 *Nucl. Fusion* **22**, 1349.
Hazeltine, R. D. & Hinton, F. L. 1973 *Phys. Fluids* **16**, 1883.
Hazeltine, R. D., Hinton, F. L. & Rosenbluth, M. N. 1973 *Phys. Fluids* **16**, 1645.
Hirshman, S. P., Hawryluk, R. J. & Birge, B. 1977 *Nucl. Fusion* **17**, 611.
Hirshman, S. P. & Sigmar, D. J. 1981 *Nucl. Fusion* **21**, 1079.
Kadomtsev, B. B. 1965 *Plasma turbulence*. New York: Academic Press.
Kadomtsev, B. B. & Pogutse, O. P. 1971 *Nucl. Fusion* **11**, 67.
Kadomtsev, B. B. 1975 *Soviet J. Plasma Phys.* **1**, 389.
Kadomtsev, B. B. 1986 In *Proc. 12th European Conference on Controlled Fusion and Plasma Physics, Budapest, 2–6 September 1985*. (*Plasma Phys. controlled Fusion* **28**, 125.)
Laing, E. W., Roberts, S. J. & Whipple, R. T. 1959 *J. nucl. Energy* C **1**, 49.
Liewer, P. C. 1985 *Nucl. Fusion* **25**, 543.
Morozov, A. I. & Solov'ev, L. S. 1966 *Reviews of plasma physics*, vol. 2, p. 1–100. New York: Consultants Bureau.
Rebut, P. H. & Brusati, M. 1986 In *Proc. 12th European Conference on Controlled Fusion and Plasma Physics, Budapest, 2–6 September 1985*. (*Plasma Phys. controlled Fusion* **28**, 113.)
Rechester, A. B. & Stix, T. H. 1976 *Phys. Rev. Lett.* **35**, 587.
Rechester, A. B. & Rosenbluth, M. N. 1978 *Phys. Rev. Lett.* **40**, 38.
Rosenbluth, M. N., Hazeltine, R. D. & Hinton, F. L. 1972 *Phys. Fluids* **15**, 116.
Shafranov, V. D. 1957 *Rev. Plasma Phys.* **2**, 116.
Spitzer, L. 1956 *Physics of Fully Ionised Gases*. New York: Interscience.
Turner, M. F. & Wesson, J. A. 1982 *Nucl. Fusion* **22**, 1069.
Ware, A. A. 1970 *Phys. Rev. Lett.* **25**, 15.
Watkins, M. L., van Maanen-Abels, A. E. P. M. & Düchs, D. F. 1984 *J. nucl. Mater.* **121**, 429.
Wesson, J. A. 1986 In *Proc. 12th European Conference on Controlled Fusion and Plasma Physics, Budapest, 2–6 September 1985*. (*Plasma Phys. controlled Fusion* **28**, 243.)

Discussion

D. C. Robinson (*UKAEA, Culham Laboratory, Abingdon, U.K.*). In his three-zone modelling Dr Bickerton appeared to assume that the profiles were flat inside the $q = 1$ surface and yet the experimental evidence suggests that the confinement inside the $q = 1$ surface is very good. Could he comment on this apparent deficiency in his model?

He also indicated that the experimental profiles were weakly tearing-mode unstable whereas the profiles predicted neoclassically were stable. Tokamak experiments indicate that the profiles are tearing-mode stable as no low-mode-number activity is observed except shortly before a disruption. Theory and experiment seem to be at variance. Could he comment on this?

R. J. Bickerton. For the experimental case treated here, which has only ohmic heating, the sawtooth amplitude is relatively small and the period is shorter than even the global confinement time (see figure 4). Thus the electron temperature profile inside the $q = 1$ surface changes very little during the sawtooth period. Under these conditions it is not possible to say whether the confinement inside the $q = 1$ surface is better or worse than the global value.

In other experiments with centralized radio-frequency heating the sawtooth amplitude and period are both much larger. For these the analysis suggests that the confinement time inside $q = 1$ is about the same as the global value.

In the sawtooth model used in our calculations the sawtooth crash is triggered when q on the axis falls below a critical value. Because there is no full understanding of the sawtooth phenomenon this critical value is tuned to give the same period as seen in the experiment. The resulting critical value of *ca.* 0.95 is physically reasonable.

In the work on tearing-mode stability the result is that one mode is weakly unstable, but a slight modification, within the errors, of the experimental profile would cause it to be stable. In addition, we used a cylindrical model for the analysis and we would expect a full toroidal treatment to show greater stability. This point serves to emphasize our conclusion that the apparently fixed current profile is not determined by marginal stability against tearing modes.

PHILOSOPHICAL TRANSACTIONS OF THE ROYAL SOCIETY A MATHEMATICAL, PHYSICAL & ENGINEERING SCIENCES